Structural phase transition and superlattice misfit strain of *R*FeAsO (*R*=La, Pr, Nd, Sm)

A. Ricci,[1] N. Poccia,[1] B. Joseph,[1] L. Barba,[2] G. Arrighetti,[2] G. Ciasca,[1] J.-Q. Yan,[3] R. W. McCallum,[3] T. A. Lograsso,[3] N. D. Zhigadlo,[4] J. Karpinski,[4] and A. Bianconi[1,*]

[1]*Dipartimento di Fisica, Università di Roma "La Sapienza," P. le Aldo Moro 2, 00185 Roma, Italy*

[2]*Institute of Crystallography, National Council of Research, Elettra, 34012 Trieste, Italy*

[3]*Divison of Materials Science and Engineering, Ames Laboratory, US-DOE, Ames, Iowa 50011, USA*

[4]*Laboratory of Solid State Physics, ETH Zurich, 8093 Zurich, Switzerland*

(Received 5 June 2010; revised manuscript received 18 September 2010; published 11 October 2010)

The tetragonal-to-orthorhombic structural phase transition (SPT) in LaFeAsO (La-1111) and SmFeAsO (Sm-1111) single crystals measured by high-resolution x-ray diffraction is found to be sharp while the *R*FeAsO (*R*=La, Nd, Pr, Sm) polycrystalline samples show a broad continuous SPT. Comparing the polycrystalline and the single-crystal 1111 samples, the critical exponents of the SPT are found to be the same while the correlation length critical exponents are found to be very different. These results imply that the lattice fluctuations in 1111 systems change in samples with different surface to volume ratio that is assigned to the relieve of the temperature-dependent superlattice misfit strain between active iron layers and the spacer layers in 1111 systems. This phenomenon that is missing in the AFe_2As_2 (*A*=Ca, Sr, Ba) "122" systems, with the same electronic structure but different for the thickness and the elastic constant of the spacer layers, is related with the different maximum superconducting transition temperature in the 1111 (55 K) versus 122 (35 K) systems and implies the surface reconstruction in 1111 single crystals.

DOI: 10.1103/PhysRevB.82.144507 PACS number(s): 74.70.Xa, 62.20.−x, 61.05.cp, 61.66.Dk

I. INTRODUCTION

The natural lattice misfit between first two-dimensional (2D) atomic monolayers and second intercalated spacer layers forming a three-dimensional (3D) superlattice, such as in intercalated graphite,[1] called the *superlattice misfit strain* (SMS) is known to be a key physical variable to describe the physics of these heterostructures at atomic limit. The SMS is of wide use in the study of multilayer semiconductor heterostructures[2] and of a variety of 3D (2D) bulk systems containing 2D (one-dimensional) interfaces.[3] For a given SMS the response of the system depends on the difference between the elastic constant of the first and the second layers, their respective temperature dependence, and the thickness of spacer layers.[4] All-known high-temperature superconductors (HTS), cuprates, diborides, and pnictides, are heterostructures at atomic limit[5] made of first atomic superconducting monolayers intercalated by second layers with variable thickness playing the role of spacers.[6,7] The SMS is a key physical variable controlling the superconducting critical temperature, T_c, at constant doping in cuprates,[8,9] diborides,[10] and pnictides.[11] Recently the complex heterogeneity in high T_c superconducting cuprates,[12] has been related to the SMS that plays a key role in these functional complex systems.[13] In pnictides[14–17] the T_c at constant doping shows very large variation as a function of the SMS that induces the deformation of the FeAs lattice, usually measured by the variation of the distance of As ion from the Fe plane.[18,19] This deformation is due to the variable SMS induced by the variable spacer material since the FeAs layer remains unchanged. The proximity to structural tetragonal-orthorhombic phase transition (SPT) in the undoped pnictides has been identified as a key feature for HTS.[20–28] The SPT precedes magnetic ordering in the parent *R*FeAsO(1111) compounds[19] whereas both transitions occur simultaneously in the AFe_2As_2(122) compounds.[20–22] For the investigation of lattice effects in HTS, it is of high interest to understand the variation in the lattice response as function of the elastic constant and thickness of the spacer layers in the proximity of the SPT.[29] The SMS is expected to induce a microstrain in the active layers that develops a complex lattice structure.[1–4] The initial studies on the 122 systems indicated the dynamic crystal symmetry breaking to be a second-order phenomena,[20] however, later studies tend to support a picture of a weakly first-order transition[22] and this topic is an object of active investigation.[30,31] Here, using high-quality single crystals together with corresponding polycrystalline powder samples, we have measured the SPT in the 1111 systems using high-resolution synchrotron x-ray diffraction study of the diffraction intensities and the line-shape broadening.

II. EXPERIMENTAL METHODS

The single crystals of the 1111 systems are more unstable and difficult to synthesize compared to the 122 compounds. A general method adopted for the synthesis of the 1111 single crystals is using the cubic anvil high-pressure technique.[32,33] Single crystals of SmFeAsO used in this study were grown under high pressure in NaCl flux[32,33] while LaFeAsO single crystals were grown under ambient pressure in NaAs flux.[34] We have used one of the best available Sm-1111 single crystals which have around 60 μm$\times$60 μm surface area with $\sim$10 μm thickness. Compared to this the La-1111 single crystal was larger with around 2 mm $\times$2 mm surface area and $\sim$10 μm thickness. The *R*FeAsO (*R*=La, Nd, Pr, Sm) polycrystalline samples were prepared by high-pressure synthesis method.[16] The x-ray diffraction (XRD) data on the single crystal samples were obtained at ELETTRA synchrotron radiation facility, Trieste.

The data were collected in the *K* geometry with a photon energy of 12.4 keV using a 2D charged couple device x-ray detector. The sample temperature was varied between 4 and 300 K, and stabilized at the set point waiting for a temperature gradient in the sample to be less than 0.1 K. All the images measured by single-crystal diffraction were properly processed using FIT2D program. The XRD measurements on the polycrystalline powder samples were performed at the Swiss light source facility at PSI, Zurich. The energy resolution was 0.014% with photon wavelength $\lambda = 0.495926$ Å. Data analysis were performed with the GSAS suite of Rietveld analysis programs.

III. RESULTS AND DISCUSSIONS

Figure 1 shows the temperature-dependent variation in the unit-cell constants, *a* and *b*, during the cooling and warming cycles for the La-1111 and Sm-1111 single-crystals and polycrystalline powders, respectively. The high-resolution x-ray diffraction profile of the 220 reflection of the high-temperature tetragonal structure ($P4/nmm$ space group) and the 040 and 400 lines of the low-temperature orthorhombic phase (*Cmma* space group) of the investigated pnictides are shown in Fig. 1. To make quantitative analysis, involving the relative intensities and full width at half maximum (FWHM), the peaks were deconvoluted with Gaussian functions. As one lower the temperature, the diffraction profiles get broader and finally split into two distinct peaks clearly indicating the SPT (Fig. 1). The nature of the SPT in the single crystals and corresponding polycrystalline powders is described by the order parameter $\mathrm{OP} = [(a-b)/(a+b)] \times 10^3$, where *a* and *b* are the lattice constants. In Fig. 1 lower panel, we compare the order parameter (OP) of the single-crystal samples with the polycrystalline powders. Furthermore, the upper insets in all the upper and middle panels of Fig. 1, clearly indicate the presence of a hysteresis of the structural phase transition in the 1111 systems.

The order parameter of the single crystals are sharper than the corresponding polycrystalline powders in its approach toward the SPT critical temperature, T_s. The data corresponding to both single crystal and polycrystalline powder are found to follow a power law with the same critical exponent, β and values 0.25 ± 0.02 for La-1111 and 0.19 ± 0.02 for Sm-1111, respectively. In comparison, the onset of the orthorhombic order is reported to have the β values 0.103 ± 0.018 and 0.112 ± 0.01 in $BaFe_2As_2$ and $EuFe_2As_2$, respectively.[20–22] In fact the same analysis, taking the data from the literature, for the $BaFe_2As_2$ yields a value 0.136 ± 0.02 (Fig. 1, inset in the lower panel). The difference between the critical exponents of La-1111 and Sm-1111 from the $(Ba,Eu)Fe_2As_2$ is an index of a different structural coupling of the electronic and lattice strain degrees of freedom in the 1111 and 122 families.[35] The critical exponent of the La-1111 system is $\beta = 0.25$, which is quite different from the mean field calculation of the critical exponent $\beta = 0.5$. The $\beta = 0.194$ found in Sm-1111 is still lower than 0.25 found in La-1111.

A comparison of the variation in the intensity of the 220 peak before and after the SPT, for the single-crystals and polycrystalline powders show remarkable differences, shown in the upper panel of Fig. 2. As evident from the intensity variation, the SPT occurs over an extended temperature range of about 90 K for the polycrystalline powders, whereas the SPT process is confined within a window of around 20 K in single crystals. Upon cooling-warming cycles, a similar temperature hysteresis, as seen in the lattice constant, is also

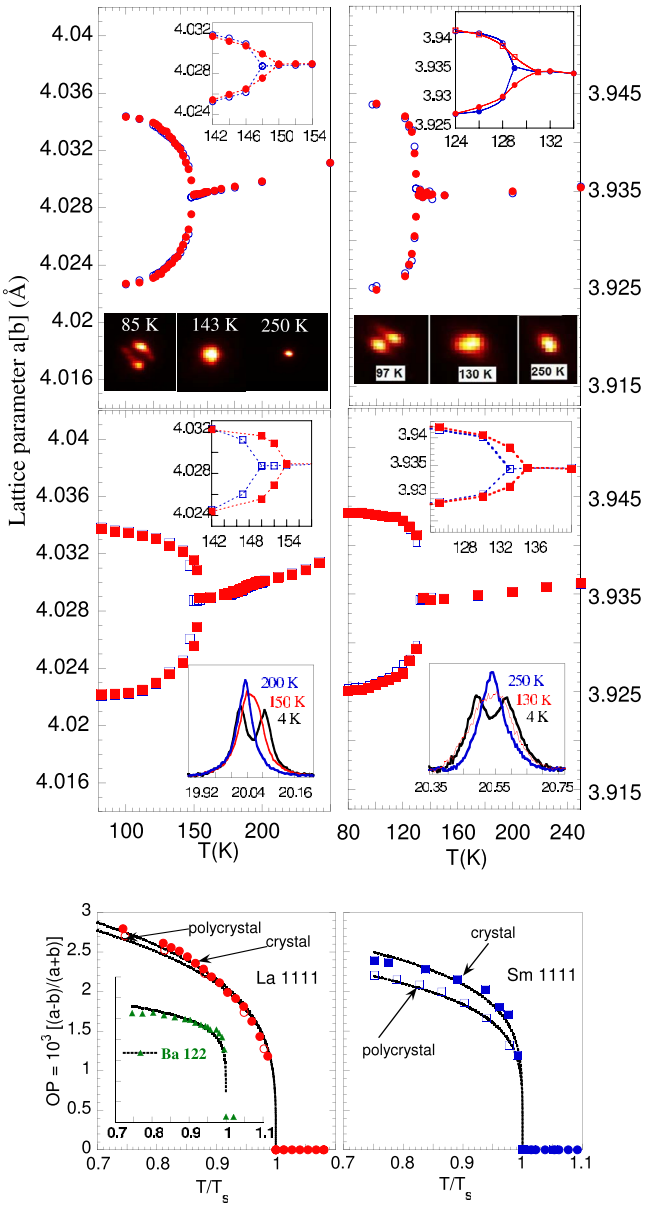

FIG. 1. (Color online) Upper panels show a (b) lattice constant of the LaFeAsO (left) and SmFeAsO (right) single-crystal samples as a function of temperature during cooling (empty blue circles) and warming (filled red circles) cycle. Middle panels show the same for the corresponding polycrystalline powder samples. Upper insets in these panels show the zoomed region over the SPT indicating the presence of a hysteresis whereas the lower insets in these panels show the evolution of the 220 spot/peak during cooling. Lower panel presents the order parameters for the single crystals and polycrystalline powders during cooling. The order parameter of the $BaFe_2As_2$ system taken from Ref. 22 is shown in the inset for comparison.

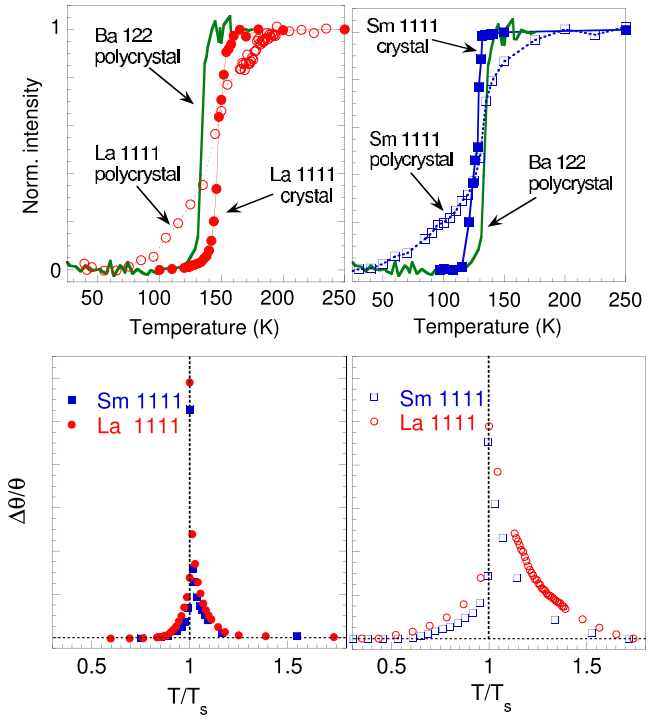

FIG. 2. (Color online) Upper panel: intensity variation of the 220 peak as a function of temperature for the single crystal and polycrystalline powder samples of LaFeAsO (marked as La 1111) and SmFeAsO (marked as Sm 1111) systems together with the intensity variation in a similar peak observed in the $BaFe_2As_2$ system (marked as Ba 122 polycrystalline powder). Lower panel: $\Delta\theta/\theta$ of the 220 peak in the tetragonal phase and 400 peak in the orthorhombic phase as a function of T/T_s for the Sm-1111 and La-1111 single crystals (left panel) and polycrystalline powders (right panel). Size of dots shows the dimension of error bar.

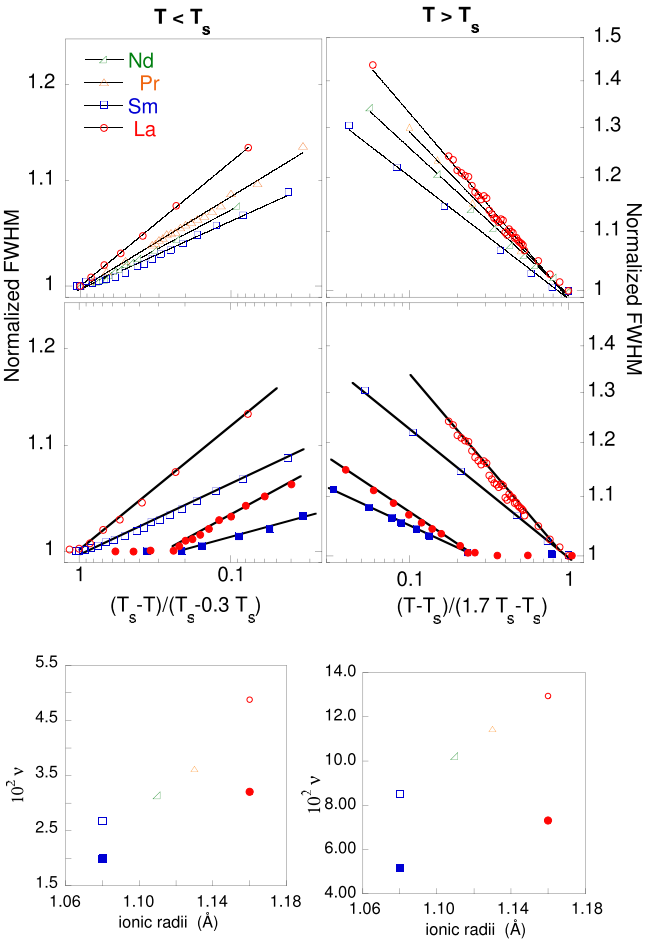

FIG. 3. (Color online) Normalized FWHM of the tetragonal 220 peak and corresponding orthorhombic 400 (or 040) peak as a function of temperature for the *R*FeAsO (*R*=La, Pr, Sm, Nd) systems. $T<T_s$ and $T>T_s$ are shown in the left and right panels, respectively. Upper panel compares the behavior of the polycrystalline powder samples. Middle panels compare the normalized FWHM of the single-crystal and polycrystalline powder systems. Fit to the data are included as lines. The exponents obtained from the fits are compared in the lower panels as a function of the rare-earth ionic size. Size of dots shows the dimension of error bar.

seen in the intensity plots (not shown). From Fig. 2, it is clear that the SPT behavior in 1111 single crystals and 122 systems are quite similar. As one approaches the structural transition temperature, the polycrystalline sample due to its finite size increasingly becomes vulnerable to the lattice fluctuations leading to an overall broadening of the transition region, resulting in an effective increase in the T_s values of the polycrystalline powders compared to single crystals (see Fig. 2). The fact that this effect is seen only in the 1111 systems, and not in the 122, implies that the origin of this effect is due to the presence of the spacer layer in the former. The large difference of the lattice fluctuations near a structural phase transition of 1111 samples with different surface to volume ratio show a lattice instability much bigger compared to the 122 systems. It is instructive to compare the evolution of the FWHM of the tetragonal 200 peak and the corresponding orthorhombic peaks (400 or 040), which is shown in Fig. 2 lower panel. Approaching the T_s, the FWHM has longer tail for polycrystalline powder than in single-crystal samples. It is in fact well known that the widths of diffraction lines are inverse to the sizes of crystallites formed during the material synthesis and that these lines are broadened by microstrain.[4,36] The difference in the SPT behavior in the single crystal and polycrystalline powder can be understood invoking the idea of larger crumbling of the microcrystallites of the polycrystalline 1111 samples in comparison to the single crystals as one approaches the SPT temperature.

In Fig. 3, we plot the normalized FWHM with the normalized temperature for the polycrystalline powders and single crystals. The results for the PrFeAsO and NdFeAsO polycrystalline powder samples are also shown. For temperature below T_s, the normalization is done by taking the value of the FWHM at $0.3\times T_s$ to unity (Fig. 3 lower panel), while for temperatures above T_s, the normalization is done by taking the FWHM values at $1.7\times\ T_s$ to unity. The correlation length ξ (has an inverse relation with FWHM, see Refs. 37 and 38) of the line-shape approaching T_s is well described by a power law $\xi^{-1}=t^{\nu}$, where t is the reduced temperature (defined in Fig. 3). Although both single crystals and polycrystalline powders are found to follow the $\xi^{-1}=t^{\nu}$ power law, the corresponding exponent, ν, for the polycrystalline powder

and the single crystal are found to be very different for the identical system, the later being four times higher. Such powder-law fits for the polycrystalline powders of La-1111, Pr-1111, Sm-1111, and Nd-1111 are shown in the upper panels of Fig. 3. In the case of the polycrystalline powder samples, the exponent increases almost linearly with increasing rare-earth ionic size (see Fig. 3 lower panels). Marked difference in the correlation length exponents observed in the case of the polycrystalline powder and the corresponding single crystals is an evidence of the crystallite size-dependent SMS effects in the 1111 system. However both 1111 materials (grown with two different procedures) show different lattice fluctuations going from microcrystallines of powders (diameter less than 1μ) to larger single crystals. The difference between the small grains and large single crystals is attributed to the difference between the elastic constant of active FeAs and rare-earth oxide spacer layers. In 1111 polycrystalline systems the surface of grains is expected to be different since the surface layer has a different elastic strain compared to the layers in the bulk. On the contrary, the 122 systems show similar lattice response for the small (polycrystalline powder) and for large crystals indicating that the surface to volume ratio does not play a significant role in 122 systems and the elastic stress due to the natural interlayer misfit is different. This difference in the lattice response could be related to the unexplained difference of the superconducting critical temperature between 1111 and 122 samples having similar electronic structure.

IV. CONCLUSIONS

In conclusion, the structural phase transition in the La-1111 and Sm-1111 appears to be a case of intermixing of first- and second-order transitions that in correlated materials is not rare. The comparison between the x-ray diffraction data for the polycrystalline 1111 samples and the single crystals shows a relevant differences as one approach the SPT temperature. This is assigned to an elastic response dependence of the surface to volume ratio of the sample. Difference in the β exponent and the temperature dependence of the single crystal and polycrystalline powder data underline the importance of the superlattice misfit strain[8,13] in the phase diagram and for the functional properties[12] of these heterostructures at atomic limit. The 122 systems on the contrary show the same lattice fluctuations in microcrystals and large crystals. This difference (between the 1111 and 122) is assigned to the difference between the elastic constant of the spacer layers in the two systems. The electronic structure of 1111 and 122 systems is very similar so this difference in the dynamical response between the 1111 and 122 systems may explain the increase in the T_c, from 35 K in 122 to 55 K in 1111 systems in fact the misfit strain has been proposed to be the key term determining the critical multiscale phase separation in doped high-temperature superconductors giving the so-called superstripes scenario.[13,39]

ACKNOWLEDGMENTS

We thank Z.-A. Ren and Z.-X. Zhao for providing the powder samples, the X04SA beamline staff of Swiss light source, Zurich, for help, the Paul Scherrer Institute, Zurich, for support of European researchers, and N. L. Saini for discussions. This project is supported by the Sapienza University of Rome. The work at the ETH Zurich was supported by the Swiss National Science Foundation through the NCCR pool MaNEP. Ames laboratory is operated for U.S. Department of Energy by Iowa State University under Contract No. DE-AC02-07CH11358.

*Corresponding author; antonio.bianconi@roma1.infn.it

[1] P. Bak, Rep. Prog. Phys. **45**, 587 (1982).
[2] S. C. Jain, A. H. Harker, and R. A. Cowley, Philos. Mag. A **75**, 1461 (1997).
[3] G. Forgacs, R. Lipowsky, and Th. M. Nieuwenhuizen, *Phase Transitions and Critical Phenomena*, edited by C. Domb and J. L. Lebowitz (Academic Press, London, UK, 1991), Vol. 14, p. 135.
[4] H. Nagao and N. Aikawa, J. Am. Ceram. Soc. **71**, C421 (1988).
[5] A. Bianconi, Solid State Commun. **89**, 933 (1994).
[6] A. Bianconi, European Patent No. 0733271 (7 December 1993).
[7] A. Ricci, B. Joseph, N. Poccia, W. Xu, D. Chen, W. S. Chu, Z. Y. Wu, A. Marcelli, N. L. Saini, and A. Bianconi, Supercond. Sci. Technol. **23**, 052003 (2010).
[8] A. Bianconi, G. Bianconi, S. Caprara, D. D. Castro, H. Oyanagi, and N. L. Saini, J. Phys.: Condens. Matter **12**, 10655 (2000).
[9] N. Poccia and M. Fratini, J. Supercond. Novel Magn. **22**, 299 (2009).
[10] S. Agrestini, N. L. Saini, G. Bianconi, and A. Bianconi, J. Phys. A **36**, 9133 (2003).
[11] A. Ricci, N. Poccia, G. Ciasca, M. Fratini, and A. Bianconi, J. Supercond. Novel Magn. **22**, 589 (2009).
[12] E. Dagotto, Science **309**, 257 (2005).
[13] M. Fratini, N. Poccia, A. Ricci, G. Campi, M. Burghammer, G. Aeppli, and A. Bianconi, Nature (London) **466**, 841 (2010).
[14] N. Poccia, A. Ricci, and A. Bianconi, Adv. Condens. Matter. Phys. (2010), 261849.
[15] T. Egami, B. V. Fine, D. Parshall, A. Subedi, and D. J. Singh, Adv. Condens. Matter. Phys. (2010), 164916.
[16] Z.-A. Ren and Z.-X. Zhao, Adv. Mater. **21**, 4584 (2009).
[17] D. Gioacchino, A. Marcelli, S. Zhang, M. Fratini, N. Poccia, A. Ricci, and A. Bianconi, J. Supercond. Novel Magn. **22**, 549 (2009).
[18] Y. Mizuguchi, Y. Hara, K. Deguchi, S. Tsuda, T. Yamaguchi, K. Takeda, H. Kotegawa, H. Tou, and Y. Takano, Supercond. Sci. Technol. **23**, 054013 (2010).
[19] J. Zhao *et al.*, Nature Mater. **7**, 953 (2008).
[20] M. Tegel, M. Rotter, V. Wei, F. M. Schappacher, R. Pšttgen, and D. Johrendt, J. Phys.: Condens. Matter **20**, 452201 (2008).
[21] N. Ni, S. Nandi, A. Kreyssig, A. I. Goldman, E. D. Mun, S. L. Bud'ko, and P. C. Canfield, Phys. Rev. B **78**, 014523 (2008).
[22] S. D. Wilson, C. R. Rotundu, Z. Yamani, P. N. Valdivia, B.

Freelon, E. B. Courchesne, and R. J. Birgeneau, Phys. Rev. B **81**, 014501 (2010).
[23] S. D. Wilson, Z. Yamani, C. R. Rotundu, B. Freelon, E. B. Courchesne, and R. J. Birgeneau, Phys. Rev. B **79**, 184519 (2009).
[24] T. Nomura, S. W. Kim, Y. Kamihara, M. Hirano, P. V. Sushko, K. Kato, M. Takata, A. L. Shluger, and H. Hosono, Supercond. Sci. Technol. **21**, 125028 (2008).
[25] S. Margadonna, Y. Takabayashi, M. T. McDonald, M. Brunelli, G. Wu, R. H. Liu, X. H. Chen, and K. Prassides, Phys. Rev. B **79**, 014503 (2009).
[26] M. Fratini *et al.*, Supercond. Sci. Technol. **21**, 092002 (2008).
[27] Y. Luo *et al.*, Phys. Rev. B **80**, 224511 (2009).
[28] A. Jesche, C. Krellner, M. de Souza, M. Lang, and C. Geibel, Phys. Rev. B **81**, 134525 (2010).
[29] A. Ricci, M. Fratini, and A. Bianconi, J. Supercond. Novel Magn. **22**, 305 (2009).
[30] M. S. da Luz, J. J. Neumeier, R. K. Bollinger, A. S. Sefat, M. A. McGuire, R. Jin, B. C. Sales, and D. Mandrus, Phys. Rev. B **79**, 214505 (2009).
[31] N. Kaurav, Y. T. Chung, Y. K. Kuo, R. S. Liu, T. S. Chan, J. M. Chen, J.-F. Lee, H.-S. Sheu, X. L. Wang, S. X. Dou, S. I. Lee, Y. G. Shi, A. A. Belik, K. Yamaura, and E. Takayama-Muromachi, Appl. Phys. Lett. **94**, 192507 (2009).
[32] J. Karpinski, N. D. Zhigadlo, S. Katrych, Z. Bukowski, P. Moll, S. Weyeneth, H. Keller, R. Puzniak, M. Tortello, D. Daghero, R. Gonnelli, I. Maggio-Aprile, Y. Fasano, O. Fischer, K. Rogacki, and B. Batlogg, Physica C **469**, 370 (2009).
[33] N. D. Zhigadlo, S. Katrych, Z. Bukowski, S. Weyeneth, R. Puzniak, and J. Karpinski, J. Phys.: Condens. Matter **20**, 342202 (2008).
[34] J. Q. Yan, S. Nandi, J. L. Zarestky, W. Tian, A. Kreyssig, B. Jensen, A. Kracher, K. W. Dennis, R. J. McQueeney, A. I. Goldman, R. W. McCallum, and T. A. Lograsso, Appl. Phys. Lett. **95**, 222504 (2009).
[35] C. Krellner, N. C. Canales, A. Jesche, H. Rosner, A. Ormeci, and C. Geibel, Phys. Rev. B **78**, 100504 (2008).
[36] F. Frey, in *Local Structure from Diffraction*, edited by S. J. L. Billinge and M. F. Thorpe (Plenun, New York, 2002), pp. 295–321.
[37] M. E. Fisher, Rep. Prog. Phys. **30**, 615 (1967).
[38] A. L. Patterson, Phys. Rev. **56**, 978 (1939).
[39] A. Bianconi, D. Di Castro, N. L. Saini, and G. Bianconi, in *Phase Transitions and Self-Organization in Electronic and Molecular Networks*, Fundamental Materials Research, edited by M. F. Thorpe and J. C. Phillips (Kluwer Academic, Boston, 2002), Chap. 24, pp. 375–388.